JOURNAL OF VIROLOGY, Mar. 2010, p. 2636–2647 Vol. 84, No. 6
0022-538X/10/$12.00 doi:10.1128/JVI.01991-09

Evidence for Multiple Recent Host Species Shifts among the Ranaviruses (Family *Iridoviridae*)▽†

James K. Jancovich,[1] Michel Bremont,[2] Jeffrey W. Touchman,[3] and Bertram L. Jacobs[1,3]*

The Biodesign Institute, Arizona State University, Tempe, Arizona 85287-5401[1]; Unité de Virologie et Immunologie Moléculaires, Institut National de la Recherche Agronomique, F-78352 Jouy-en-Josas, France[2]; and School of Life Sciences, Arizona State University, Tempe, Arizona 85287-4601[3]

Received 21 September 2009/Accepted 18 December 2009

Members of the genus *Ranavirus* (family *Iridoviridae*) have been recognized as major viral pathogens of cold-blooded vertebrates. Ranaviruses have been associated with amphibians, fish, and reptiles. At this time, the relationships between ranavirus species are still unclear. Previous studies suggested that ranaviruses from salamanders are more closely related to ranaviruses from fish than they are to ranaviruses from other amphibians, such as frogs. Therefore, to gain a better understanding of the relationships among ranavirus isolates, the genome of epizootic hematopoietic necrosis virus (EHNV), an Australian fish pathogen, was sequenced. Our findings suggest that the ancestral ranavirus was a fish virus and that several recent host shifts have taken place, with subsequent speciation of viruses in their new hosts. The data suggesting several recent host shifts among ranavirus species increase concern that these pathogens of cold-blooded vertebrates may have the capacity to cross numerous poikilothermic species barriers and the potential to cause devastating disease in their new hosts.

Iridoviruses are large, double-stranded DNA viruses that infect both vertebrate and invertebrate hosts (9, 64). The family *Iridoviridae* currently contains five genera, the *Iridovirus* and *Chloriridovirus* genera, associated with insects, the *Lymphocystivirus* and *Megalocytivirus* genera, which infect fish species, and the genus *Ranavirus*, whose members have been associated with mortality events in amphibians, fish, and reptiles (64). At this time, the type isolates for each genus in the family *Iridoviridae* have been sequenced (Table 1).

Members of the genus *Ranavirus* have been recognized as major pathogens of economically and ecologically important cold-blooded vertebrates (8, 64). For example, ranaviruses (RVs) have been isolated from amphibians in North America (6, 18, 24, 34, 35), Asia (27, 66), Australia (56), and the United Kingdom (10, 19), from fish (2, 41, 46), and from reptiles (3, 14, 30, 37, 42, 43). In fact, ranaviruses are now considered agents of emerging infectious disease (9). As interest in RVs has grown, the number of ranaviruses that have been completely sequenced has also increased. These include frog virus 3 (FV3) (58), the type virus of the genus *Ranavirus*; tiger frog virus (TFV) (27), an RV closely related to FV3 that was isolated from frogs in Asia; and *Ambystoma tigrinum* virus (ATV) (36), an RV associated with salamander mortalities in North America. In addition, two grouper iridoviruses which are also members of the genus *Ranavirus*, the grouper iridovirus (GIV) (62) and the Singapore grouper iridovirus (SGIV) (53), were recently sequenced. In addition, at the time of preparation of the manuscript, the genomic sequence of the soft-shelled turtle ranavirus (STIV) became available (29). Information obtained by comparing ranavirus genomic sequences offers insight into RV evolutionary history, identifies core groups of genes, and gives insight into the genes responsible for viral immune evasion and pathogenesis.

Previous studies have shown that RV isolates can be translocated across large distances in infected salamanders that are used as bait for sport fishing (35, 44, 51). Phylogenetic analysis was used to compare the major capsid protein (MCP) sequences from salamander RV isolates from the southern Arizona border to Canada to other RV MCP sequences (35). The data suggest that salamander RV isolates are more closely related to fish RV isolates, such as epizootic hematopoietic necrosis virus (EHNV), than to other amphibian (frog) RV isolates, such as FV3 (35). Dot plot analysis comparing the genomic sequence of ATV to those of FV3 and TFV showed two major genomic inversions (36), while the FV3 and TFV genomes showed complete colinearity. These data suggest that at some point in virus evolutionary history, an ancestral virus diverged into the salamander virus and frog virus lineages. A genomic rearrangement occurred in one of the lineages at the time of divergence or after. Subsequent host-specific evolution occurred, limiting cross transmission among isolates, in such a way that frog RVs do not cause disease during laboratory infection of salamanders and vice versa (34). There is some evidence that salamander RV isolates can be isolated from or detected in laboratory-infected frogs (52) and that a pathogen host shift is the result of the movement of these pathogens (35). Thus, the ecological and economic consequences of RVs moving in the environment include the potential of these pathogens infecting and decimating new amphibian, fish, or reptile populations. Therefore, a more complete understanding of the genetic determinants that make up RVs would help to predict future transmission events.

EHNV was isolated in Australia from redfin perch (*Perca fluviatilis*) and rainbow trout (*Oncorhynchus mykiss*) (38, 39).

* Corresponding author. Mailing address: School of Life Sciences, Arizona State University, Tempe, AZ 85287-4601. Phone: (480) 965-4684. Fax: (480) 727-7615. E-mail: bjacobs@asu.edu.

† Supplemental material for this article may be found at http://jvi.asm.org/.

▽ Published ahead of print on 30 December 2009.

TABLE 1. Completely sequenced iridoviruses

Genus	Virus	Known host	Genome size (kb)	GC content (%)	No. of potential genes	GenBank accession no.
Ranavirus	ATV	Salamander	106,332	54	92	AY150217
	EHNV	Fish	127,011	54	100	FJ433873
	FV3	Frog	105,903	55	97	AY548484
	TFV	Frog	105,057	55	103	AF389451
	SGIV	Fish	140,131	48	139	AY521625
	GIV	Fish	139,793	49	139	AY666015
Megalocytivirus	ISKNV	Fish	111,362	55	117	AF371960
	OSGIV	Fish	112,636	54	116	AY894343
	RBIV	Fish	112,080	53	116	AY532606
Lymphocystivirus	LCDV-1	Fish	102,653	29	108	L63545
	LCDV-C	Fish	186,247	27	178	AY380826
Iridovirus	IIV-6 (CIV)	Insect	212,482	29	211	AF303741
Chloriridovirus	IIV-3 (MIV)	Insect	190,132	48	126	DQ643392

EHNV can be classified as an indiscriminate pathogen of freshwater finfish, as it readily kills juvenile redfin perch and rainbow trout in inland water bodies throughout Australia (63). In addition, challenge experiments showed that following bath inoculation, other fish species are also susceptible to infection with EHNV, including the Macquarie perch (*Macquaria australasica*), silver perch (*Bidyanus bidyanus*), mosquito fish (*Gambusia affinis*), and mountain galaxias (*Galaxias olidus*). In contrast, Murray cod (*Maccullochella peeli*), golden perch (*Macquaria ambigua*), Australian bass (*Macquaria novemaculeata*), Macquarie perch, silver perch, and Atlantic salmon (*Salmo salar*) were susceptible only by intraperitoneal (i.p.) injection of virus. Serological surveys (A. Hyatt, unpublished data) show that redfin perch and rainbow trout can also be carriers of EHNV. Virus was reisolated from animals not showing clinical signs of disease, making them likely vehicles for the translocation and introduction of EHNV into naïve host populations. Preliminary and unpublished data have shown that i.p. inoculation of Australian frogs or the cane toad *Bufo marinus* with EHNV results in seroconversion but no signs of clinical disease (68). While EHNV has not been identified in fish populations in North America, it is possible that this pathogen could be translocated via movement of animals for food, bait, or scientific purposes, thereby infecting and potentially decimating naïve fish populations. In fact, the disease caused by EHNV is recognized by the World Organization for Animal Health (Office International Epizootics [OIE]) as a major cause of finfish mortalities (www.oie.int). In addition, both an EHNV disease in fish and a ranavirus infection in amphibians are notifiable diseases to OIE. Since the recognition of disease due to EHNV in Australia in 1986, similar systemic necrotizing iridovirus syndromes in farmed fish have been reported. These include catfish (*Ictalurus melas*) in France (European catfish virus) (45), sheatfish (*Silurus glanis*) in Germany (European sheatfish virus) (1), turbot (*Scophthalmus maximus*) in Denmark (5), and pike perch (*Stizostedion lucioperca*) in Finland (59). In addition, while EHNV has been classified as an RV, the relationship between this fish pathogen and amphibian RVs is poorly understood. Therefore, in order to better understand the relationships among RV isolates, the complete sequence of EHNV genomic DNA was determined. The characteristics of the EHNV genome, its relatedness to other iridoviruses, and insights into RV evolution are the focus of this study.

MATERIALS AND METHODS

Generation of EHNV genomic DNA library. EHNV DNA was isolated as previously described (65) from cell culture-amplified virus stocks of the original EHNV isolated in Australia (39). The EHNV shotgun library was constructed by kinetically shearing 10 μg of viral DNA in 200 μl of TE (10 mM Tris-HCl, 1 mM EDTA) buffer. The sheared DNA was ethanol precipitated, and the pellet containing DNA was end repaired using T4 DNA polymerase and Klenow polymerase, concentrated by ethanol precipitation, and quantified. BstXI adaptors were ligated to the end-repaired viral DNA and then size selected by gel electrophoresis. DNAs of 2 to 4 kbp were extracted from the gel and ligated into the pOTWI3 plasmid. Plasmid DNA was transformed into DH10B competent cells by electroporation, plated on prewarmed agar plates containing 50 μg/ml chloramphenicol, and incubated overnight at 37°C. Colonies containing plasmid were selected using automated equipment, and plasmid DNA was isolated using solid-phase reversible immobilization (SPRI) technology. Isolated plasmids were sequenced from both ends of the insert by use of automated equipment (ABI 3730XL; Applied Biosystems). Sequences were aligned and assembled using Phred/Phrap (http://www.phrap.org) and finished using standard methods, with the aid of Consed (23).

Genome annotation. The newly sequenced genome was annotated using similar procedures to those described previously (36). Using the BLASTP, BLASTX, and TBLASTX procedures (49, 50), all open reading frames (ORFs) with sequence similarity to any other closely related viral ORF and/or containing a domain(s) or homology with any known protein were identified. Identified ORFs were confirmed using the Genome Annotation Transfer Utility (GATU) (http://www.biovirus.org/), a program that uses previously annotated genomic DNA as a reference for annotating a newly sequenced genomic DNA, using all of the completely sequenced iridoviruses as reference sequences. The iridoviruses used in this analysis were as follows (also see Table 1): ATV (36), FV3 (58), TFV (27), GIV (62), SGIV (53), lymphocystis disease virus 1 (LCDV-1) (60), lymphocystis disease virus China (LCDV-C) (67), infectious spleen and kidney necrosis virus (ISKNV) (26), orange spotted grouper iridovirus (OSGIV) (40), rock bream iridovirus (RBIV) (15), insect iridovirus 6 (IIV-6) or *Chilo* iridovirus (CIV) (33), and invertebrate iridovirus 3 (IIV-3) or mosquito iridovirus (MIV) (13). The genome of a soft-shelled turtle ranavirus isolate was published during the preparation of the manuscript (29). However, due to the timing of this publication, the genomic information from this newly isolated RV was not used in our analysis. ORFs in the *Iridoviridae* family are presumed to be nonoverlapping; however, ORFs were considered overlapping if both ORFs had high sequence identity (i.e., a high BLASTP expect score) to other sequenced iridoviruses.

Phylogenetic and dot plot analysis. Concatenated iridovirus phylogenetic analysis was conducted by obtaining the homologues of the EHNV ORFs 1L (myristylated membrane protein), 7R (RNA polymerase, α subunit), 8L (NTPase/helicase), 10L (DNA repair enzyme RAD2), 11R, 13L (ICP-46), 14L (MCP), 16L (thiol oxidoreductase), 18L (thymidine kinase), 19L (PCNA), 23L (transcription elongation factor SII), 24R (RNase III), 38R (ribonucleotide reductase, small subunit), 43R (RNA polymerase β subunit), 44L (DNA polymerase), 48L (CTD-phosphotransferase), 53L (myristylated membrane protein), 62R (tyrosine kinase), 72R, 77R, 85L (D5 NTPase), 86R, 89L (serine-threonine protein kinase), 92L (ABC ATPase), 95R, and 100R (putative replication factor) from representative members of the sequenced iridoviruses (see Tables S1 and S2 in the supplemental material) in GenBank by BLASTP analysis (http://www.ncbi.nlm.nih.gov/). All sequences were concatenated using BioEdit (http://www.mbio.ncsu.edu/BioEdit/bioedit.html). The sequences were aligned and neighbor-joining analysis was conducted using MEGA4 software (57) with default options.

Phylogenetic analysis of the EHNV ORF 87L was performed by acquiring homologous sequences by BLASTP analysis (http://www.ncbi.nlm.nih.gov/). The homologous sequences used in this phylogeny were from butterfish (GenBank accession no. ACQ58597.1), Atlantic salmon (NP_001135373.1), Northern pike (ACO14357.1), zebrafish (CAM14042.1), Norway rat (NP_569084.1), Chinese hamster (BAE78431.1), house mouse (NP_034179.1), rabbit (ACO49549.1), cow (P00376.3), horse (XP_001504693.1), rhesus monkey (XP_001110551.1), human (NP_000782.1), chimpanzee (XP_001134992.1), African clawed frog (NP_001088506.1), chicken (NP_001006584.2), zebra finch (XP_002190476.1), and herpesvirus saimiri 2 (NP_040203.1). The sequences were aligned and neighbor-joining analysis was conducted using MEGA4 software (57) with default options.

Dot plots using whole genome sequences comparing all of the sequenced iridoviruses (Table 1) to EHNV were generated using JDotter (http://www.biovirus.org/) (54, 55), using the default settings.

Nucleotide sequence accession number. The EHNV sequence was deposited in the GenBank database (http://www.ncbi.nlm.nih.gov/) under accession number FJ433873.

RESULTS AND DISCUSSION

EHNV genome characteristics. An EHNV random genomic DNA library was successfully generated and produced over 1,800 EHNV-specific sequences. The sequences contributed to the assembly of the complete genomic sequence, with an average final sequence coverage of >4-fold.

The finished EHNV genomic sequence (127,011 bp) is larger than the genomes of the amphibian RVs ATV, TFV, and FV3 (average, 105,754 bp), but smaller than the genomes of the grouper RVs GIV and SGIV (average, 139,962 bp) (Table 1). In addition, the EHNV genome is larger than the genomes of the other fish pathogens ISKNV, OSGIV, and RBIV (average, 112,026 bp) but smaller than the insect viral genomes of CIV and MIV (average, 201,307 bp). The lymphocystiviruses LCDV-1 and LCDV-C have very differently sized genomes (Table 1). EHNV genomic DNA is smaller than the average of these two viral genomic sequences (average, 144,450 bp). EHNV has a similar G+C content (54%) to those of TFV, FV3, ATV, ISKNV, OSGIV, and RBIV (53 to 55%), a slightly higher G+C content than those of the grouper iridoviruses GIV and SGIV and the insect iridovirus MIV (48 to 49%), and a much higher G+C content than those of LCDV-1, LCDV-C, and CIV (27 to 29%).

Open reading frame analysis. One hundred ORFs are predicted for the EHNV genome, based on the annotation criteria described in Materials and Methods (Fig. 1; Table 2; see Table S1 in the supplemental material). The number of ORFs predicted for EHNV (100) is similar to the number of ORFs predicted for ATV (92) and close to the numbers of ORFs predicted for FV3 (97) and TFV (103) as well; however, all of these RVs have considerably fewer ORFs than the 139 ORFs seen in the fish RVs GIV and SGIV (Table 1). In addition, the number of EHNV ORFs is relatively close to the numbers of ORFs predicted for the other fish iridoviruses ISKNV, OSGIV, RBIV, and LCDV-1, while the numbers of ORFs in LCDV-C, CIV, and MIV are much larger, corresponding to their larger genome sizes (Table 1).

Of the 100 EHNV ORFs, 26 ORFs are conserved throughout the family *Iridoviridae* (see Tables S2 and S3 in the supplemental material). These ORFs can be defined as the core iridovirus genes, since they are present in every iridovirus sequenced to date and confirm published reports that all iridoviruses contain these 26 ORFs (20). The majority of these conserved ORFs (21/26 ORFs) have a predicted function, based on sequence homology to other characterized proteins, or have been identified based on experimental data (see Table S2 in the supplemental material). In contrast, only 4 of the 27 additional ORFs that are conserved throughout the genus *Ranavirus* have a predicted function (see Tables S1 and S4 in the supplemental material), and only 1 of the 13 amphibian RV-specific genes has a predicted function (the viral homologue of eukaryotic translation initiation factor 2α [vIF2αH; ORF 61R]) (see Table S5 in the supplemental material).

Interestingly, there are three unique EHNV ORFs, namely, ORFs 64R and 65R, which have no homology to any known protein sequence, and ORF 87L, which is predicted to encode a dihydrofolate reductase (DHFR) (Table 2; see Table S1 in the supplemental material). DHFRs are thought to be involved in nucleotide metabolism and have been described for herpesviruses (61). BLAST search analysis of the EHNV ORF 87L showed the highest sequence similarity with butterfish, Atlantic salmon, and northern pike DHFRs (data not shown). Phylogenetic analysis of this EHNV ORF compared to homologous sequences suggests that EHNV acquired this unique gene from a fish host, thereby allowing the virus to replicate and cause disease in finfish (Fig. 2). There is evidence of host-derived gene transfer in poxviruses (7), a group of closely related DNA viruses (31, 32), so it is reasonable to hypothesize that similar events have occurred with iridoviruses. In fact, iridoviruses may have a higher rate of horizontal gene transfer from their host due to the nuclear stage of iridovirus DNA replication (9, 64).

There appear to be nine ORF clusters, containing a minimum of four consecutively oriented ORFs (COOs), throughout the genome. These clusters of COOs all have similar orientations, either right or left, with the majority of the COOs having the same orientation. While the genomes of iridoviruses are circularly permuted and terminally redundant (64), and therefore the orientation of these ORFs relative to the orientation of the start of the genome was an arbitrary decision, the amount of conservation among RV isolates within these regions is surprising. For example, the region between EHNV ORFs 54 and 77 contains 21 of the 24 predicted ORFs in the right orientation, while in ATV 19 of the 20 ORFs in this region (ATV ORFs 52 to 69) are oriented in the same direction (36). FV3 and TFV also have similarly oriented ORFs in this region (27, 58).

In overall appearance, the EHNV COOs are reminiscent of pathogenesis islands (PAIs) found in pathogenic bacteria. The bacterial PAIs, mobile genetic elements that contribute to rapid changes in virulence potential (16, 21, 22, 25), contain

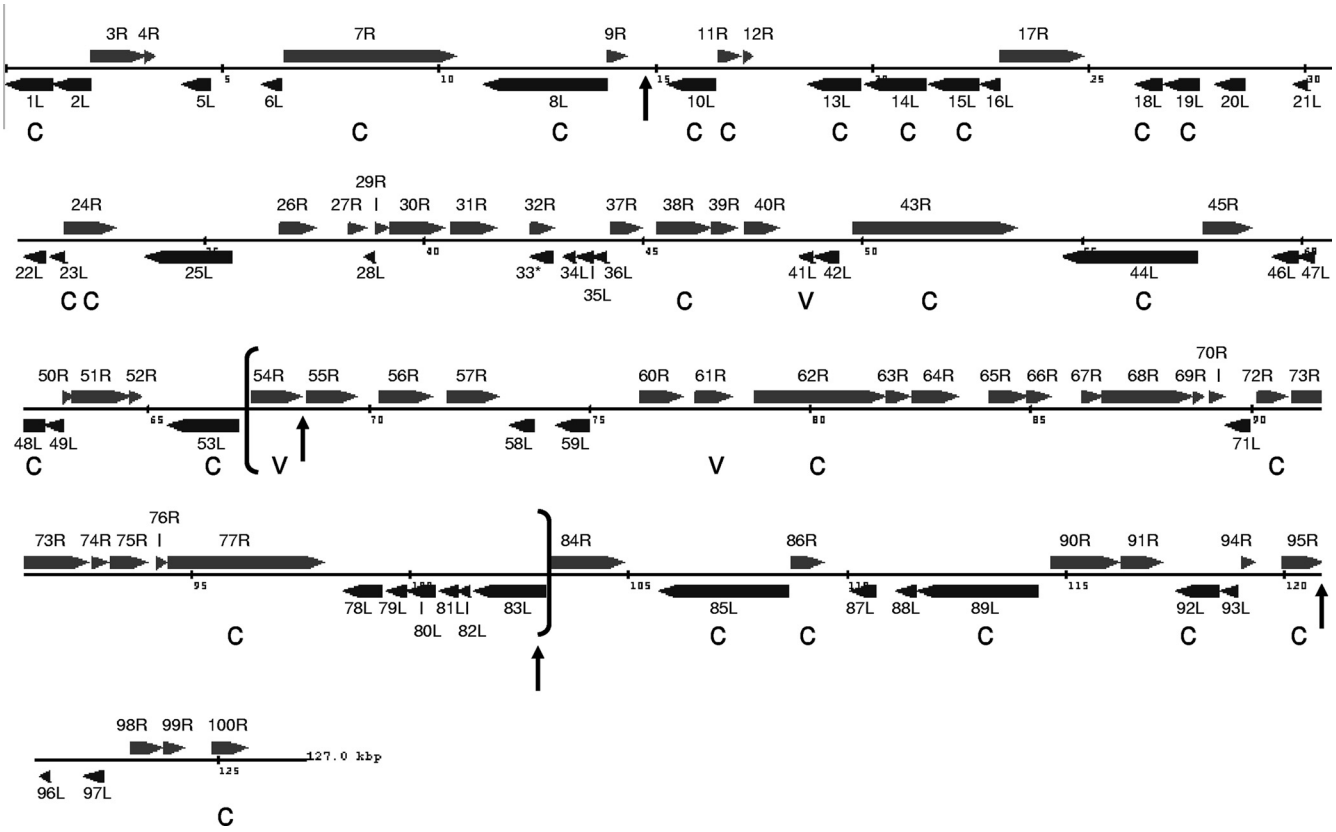

FIG. 1. Annotation of the EHNV genome showing the order and orientation of ORFs. The EHNV genome was annotated as described in Materials and Methods. Each arrow represents an ORF in the right or left orientation. Conserved iridovirus ORFs (C) and putative virulence ORFs (V) are indicated. The brackets enclose the region of consecutively oriented ORFs and the arrows indicate the locations of genomic inversions compared to FV3.

ORFs that are in the same orientation and code for proteins that have been correlated with increased pathogenesis. Poxviruses contain groups of ORFs at the hairpin ends of their genomes that are associated with virulence and have been suggested to be analogous to PAIs (11). It is interesting to note the similarity between these related vertebrate pathogens in that ORFs correlating with pathogenesis are in close proximity to each other. Further analysis of this region may help to shed light on the specific function of these ORFs.

Another interesting region of the EHNV genome is between ORFs 55R and 59L. The five ORFs within this region share homology with two ORFs from ATV (53R and 54R) and two ORFs from FV3 and TFV (23R and 24R), as well as sharing homology with each other (see Table S1 in the supplemental material). In addition, these EHNV ORFs also share homology with SGIV and GIV ORFs. EHNV 57R has homology with GIV 53L, while EHNV 56R has homology to five GIV ORFs (GIV ORFs 50L, 51L, 53L, 91L, and 94L) (see Table S1 in the supplemental material). Alignments of these EHNV ORFs (data not shown) suggest that these five EHNV ORFs may be the result of gene duplication events.

Phylogenetic analysis. Twenty-six EHNV ORFs, the core iridovirus genes, and the orthologous genes from the 12 completely sequenced iridoviruses were used to generate a concatenated phylogeny (Fig. 3). The phylogenetic tree shows high bootstrap support (100%) for EHNV being a member of the genus *Ranavirus* in the family *Iridoviridae*. In addition, EHNV is more closely related to ATV, a salamander RV, than it is to FV3 and TFV, which are frog RVs, supporting previously published analysis (35). EHNV is more distantly related to LCDV-1 and LVDC-C, to ISKNV, to OSGIV, and to RBIV, MIV, and CIV (members of the *Lymphocystivirus*, *Megalocytivirus*, *Chloriridovirus*, and *Iridovirus* genera, respectively). The grouper iridoviruses GIV and SGIV are clearly more divergent from the ATV/EHNV and FV3/TFV ranaviruses. Based on these data and that of others (53, 62), the grouper iridoviruses or GIV-like isolates could be considered a distantly related species within the genus *Ranavirus*, or perhaps a subspecies of ranaviruses. Therefore, we suggest that the RVs be divided into two subspecies, the GIV-like RV and the amphibian-like ranavirus (ALRV) subspecies, based on our observations and those of others (20). The ALRVs can then be classified further as being ATV-like or FV3-like. It is interesting that the branch lengths of the ALRVs are very short, suggesting evolutionarily recent speciation of these viral isolates.

Whole-genome alignments. Dot plot comparisons of whole genomic sequences can reveal a large amount of information on the entire genome and how genomic sequences are organized (e.g., colinearity, inversions, and repeat sequences). Comparing the sequence of EHNV to that of ATV, a −45° line can be observed (Fig. 4). Breaks in this line reveal inserted sequences, i.e., ORFs present in one genome and not in the

TABLE 2. Predicted EHNV open reading frames and best-matching iridovirus homologues

ORF[a]	Position (bp)	Size (no. of amino acids)	MW	Predicted function	Best-matching iridovirus ORF	Expect score	% Identity	% Positive	Gap %	GenBank accession no.
1L	11–1063	350	38,082	Myristylated membrane protein	FV3 2L	1e−145	98	98	0	YP_031580
2L	1101–1940	279	31,302		FV3 2.5R	6e−163	98	99	0	AY548484
3R	1970–3184	404	44,679		TFV 4R	0.0	97	99	0	ABB92272
4R	3225–3407	60	6,615		ATV 4R	8e−18	95	95	0	YP_003775
5L	4077–4715	212	24,359		FV3 6R	4e−37	97	100	0	YP_031584
6L	5931–6353	140	14,881		ATV 5L	5e−48	92	94	0	YP_003776
7R	6433–10344	1,303	141,815	RNA polymerase α subunit	ATV 6R	0.0	97	98	0	YP_003777
8L	11025–13871	948	106,432	NTPase or helicase	ATV 7L	0.0	97	98	0	AAP33184
9R	13887–14300	137	15,018		TFV 10R	2e−70	99	99	0	ABB92276
10L	15273–16367	364	40,646	DNA repair enzyme RAD2	ATV 10L	0.0	97	99	0	AAP33187
11R	16461–16928	155	17,886		ATV 11R	7e−78	97	97	0	AAP33188
12R	17041–17208	55	5,686		TFV 99L	2e−09	96	98	0	ABB92345
13L	18518–19705	395	45,578	Immediate-early protein ICP-46	FV3 91R	0.0	97	98	0	AAT09751
14L	19829–21220	463	50,105	Major capsid protein	ATV 14L	0.0	98	99	0	AAP33191
15L	21313–22419	368	41,742		TFV 95R	1e−135	79	80	14	ABB92343
16L	22487–22939	150	16,652	Thiol oxidoreductase	ATV 16L	2e−83	99	100	0	AAP33193
17R	22972–24825	617	66,505		TFV 93L	0.0	96	97	0	ABB92341
18L	26068–26655	195	22,132	Deoxyribonucleoside kinase/thymidine kinase	TFV 91.5R	7e−104	97	98	0	ABB92339
19L	26730–27512	260	27,685	Proliferating cell nuclear antigen (PCNA)	ATV 20L	3e−133	96	98	0	AAP33197
20L	27933–28577	214	24,897	Cytosine DNA methyltransferase	ATV 21L	9e−119	97	98	0	AAP33198
21L	29728–30621	297	33,872	Thymidylate synthase	ATV 22L	4e−145	94	96	0	AAP33199
22L	30900–31373	157	17,405	Putative immediate-early protein	ATV 23L	5e−89	99	100	0	AAP33200
23L	31502–31780	92	10,427	Transcription elongation factor SII	ATV 24L	8e−41	98	98	0	AAP33201
24R	31836–32954	372	40,481	RNase III	ATV 25R	0.0	98	99	0	AAP33202
25L	33681–35618	645	71,712		ATV 26L	0.0	82	85	10	AAP33203
26R*	36724–37491	255	29,090		TFV 83L	2e−118	94	95	0	ABB92336
27R	38298–38645	115	12,821		ATV 27R	1e−54	97	99	0	AAP33204
28L	38642–38863	73	7,952		ATV 28L	3e−35	98	98	0	AAP33205
29R	38926–39180	84	9,228		ATV 29R	8e−30	95	96	0	AAP33206
30R	39237–40418	393	42,021		ATV 30R	2e−164	92	95	0	AAP33207
31R	40638–41612	324	36,090	NTPase/helicase	ATV 31R	1e−177	98	99	0	AAP33208
32R	42423–42938	171	18,773		FV3 72L	8e−78	97	99	0	AAT09732
33L	42429–42911	160	17,275		TFV 77L	2e−89	98	100	0	ABB92331
34L	43196–43432	78	8,381		ATV 34L	4e−24	92	94	0	AAP33211
35L	43473–43841	122	13,201		ATV 34.5L	9e−60	95	96	1	AY150217
36L	43859–44125	88	9,360		FV3 69R	7e−37	98	98	0	AAT09729
37R	44233–44937	234	25,229		ATV 37R	6e−112	90	95	0	AAP33214
38R	45326–46489	387	44,030	Ribonucleotide reductase, small subunit	ATV 38R	0.0	98	99	0	AAP33216
39R	46547–47098	183	18,610		ATV38.5L	3e−49	96	97	0	AY150217
40R	47337–48059	240	22,522		FV3 65L	2e−07	97	97	0	AAT09725
41L	48535–48822	95	10,372	CARD-like caspase; putative interleukin-1 beta convertase	ATV 40L	7e−42	94	97	0	YP_003812
42L	48917–49411	164	17,426	dUTPase	FV3 63R	8e−79	96	98	0	YP_031642
43R	49791–53474	1227	133,829	DNA-dependent RNA polymerase, β subunit	FV3 62L	0.0	97	98	0	YP_031641
44L	54549–57590	1013	114,508	DNA polymerase	TFV 63R	0.0	99	99	0	AAL77804
45R	57756–58814	352	39,781		FV3 59L	0.0	97	98	0	YP_031638
46L	59343–59897	184	20,461		FV3 58.5R	2e−121	98	99	0	AY548484
47L	59912–60250	112	10,518		SGIV 45L	6e−11	51	59	0	YP_164140
48L	61123–62619	498	53,522	CTD-phosphotransferase	ATV 47L	0.0	97	98	0	YP_003820
49L	62661–63065	134	15,244		TFV 58R	6e−66	97	98	0	ABB92316
50R	63102–63251	49	5,208		TFV 57L	4e−09	97	100	0	ABB92315
51R	63259–64554	431	47,190	Helicase	ATV 50R	0.0	97	98	0	YP_003823
52R	64592–64822	76	8,757	Putative nuclear calmodulin-binding protein	FV3 54L	1e−29	93	96	0	YP_031632
53L	65456–67027	523	54,869	Myristylated membrane protein	ATV 51L	0.0	98	98	0	YP_003824
54R	67366–68433	355	39,399	3-β-Hydroxy-D-5-C27-steroid oxidoreductase-like protein	FV3 52L	0.0	96	98	0	YP_031630
55R	68611–69672	353	39,507		FV3 23R	7e−46	32	50	7	YP_031601
56R	70259–71407	382	42,567		FV3 23R	0.0	97	97	0	YP_031601
57R	71804–72901	365	40,928		FV3 24R	0.0	96	99	0	YP_031602
58L	73215–73724	169	19,443		FV3 23R	2e−14	31	51	4	YP_031601
59L	74255–74989	244	27,214		TFV 23R	8e−33	34	56	2	ABB92288
60R	76159–77073	304	34,545	p31K	ATV 55R	2e−148	96	98	0	YP_003828
61R	77399–78178	259	28,304	eIF2α homolog	TFV 27R	4e−134	94	96	0	AAL77798
62R	78765–81677	970	106,902	Tyrosine kinase	ATV 58R	0.0	96	98	0	YP_003831
63R	81726–82235	169	18,912		ATV 59R	8e−84	92	93	4	YP_003832
64R*	82345–83310	321	35,189	Putative capsid maturation protease (herpesvirus)						
65R*	84057–84881	275	30,740							
66R	84937–85422	161	17,937		SGIV 158L	2e−08	32	50	8	YP_164253
67R	86177–86596	139	15,143		ATV 60R	7e−73	98	99	0	YP_003833
68R	86646–88622	658	73,571	Neurofilament triplet H1-like protein	TFV 33R	0.0	80	83	10	ABB92295
69R	88707–88898	63	6,613		TFV 34R	8e−12	95	96	0	ABB92296
70R	89046–89369	107	11,546		ATV 62.5R	9e−70	97	98	0	AY150217
71L	89432–89932	166	17,840		FV3 35L	7e−66	94	94	0	ABB92299

Continued on following page

TABLE 2—*Continued*

ORF[a]	Position (bp)	Size (no. of amino acids)	MW	Predicted function	Best-matching iridovirus ORF	Expect score	% Identity	% Positive	Gap %	GenBank accession no.
72R	90144–90779	211	23,478		TFV 40R	1e−109	98	99	0	ABB92302
73R	90918–92615	565	62,186	Ribonucleotide reductase, large subunit	TFV 41R	0.0	98	99	0	AAL77800
74R	92722–93072	116	12,710		TFV 42R	6e−39	93	95	0	ABB92303
75R	93161–93967	268	28,876		ATV 67R	1e−62	76	79	5	YP_003841
76R	94224–94409	61	7,474		ATV 68R	2e−−08	72	72	24	YP_003842
77R	94481–97978	1165	129,034		ATV 69R	0.0	97	98	0	YP_003843
78L	98486–99343	285	29,429		TFV 46L	5e−74	69	70	21	ABB92307
79L	99469–99879	136	15,551		TFV 47L	2e−−72	99	100	0	ABB92308
80L	99933–100544	203	23,004	Neurofilament triplet H1-like protein	ATV 72L	4e−36	65	70	26	YP_003846
81L	100670–101086	138	15,572		FV3 47L	1e−−60	97	99	0	YP_031625
82L	101089–101340	83	9,547		TFV 50L	9e−−35	96	98	0	ABB92310
83L	101459–103084	541	60,677		ATV 75L	5e−147	77	83	5	YP_003850
84R	103165–104850	561	61,508		ATV 76R	0.0	97	99	0	YP_003851
85L	105693–108614	973	108,742	D5 family NTPase	FV3 22R	0.0	98	99	0	ABB92287
86R	108744–109403	219	25,327		ATV 78R	1e−104	99	99	0	YP_003853
87L*	110079–110648	189	21,084	Dihydrofolate reductase						
88L	111114–111563	149	16,142		ATV 79L	1e−62	97	97	0	YP_003854
89L	111611–114334	907	98,760	Serine/threonine protein kinase	TFV 19R	0.0	88	89	7	ABB92284
90R	114659–116167	502	53,345		ATV 81R	0.0	99	99	0	YP_003856
91R	116276–117151	291	31,665		ATV 82.5L	9e−147	96	98	0	YP_003857
92L	117540–118466	308	34,686	ABC-ATPase	ATV 83L	3e−178	98	98	0	YP_003858
93L	118563–118919	118	13,354		FV3 14R	3e−44	97	98	0	YP_031592
94R	119046–119288	80	9,267		ATV 85.5L	4e−31	91	96	0	YP_003860
95R	119947–120840	297	32,649		ATV 87R	2e−132	96	98	0	YP_003862
96L	120906–121118	70	7,885		ATV 88L	9e−24	95	98	0	YP_003863
97L	121917–122354	145	16,101		LCDV-C 71L	0.22	29	52	6	YP_073578
98R	123028–123714	228	24,474		ATV 89R	8e−121	96	97	0	YP_003864
99R	123780–124193	137	15,166		ATV 90R	3e−70	94	97	0	YP_003865
100R	124882–125652	256	29,693	Putative replication factor	FV3 1R	5e−144	98	98	0	YP_031579

[a] *, EHNV-specific ORFs.

other (Fig. 4; see Table S1 in the supplemental material). In addition, repeated "dots" can be seen running vertically and horizontally throughout the dot plot (Fig. 4). Interestingly, one can almost map out the EHNV ORFs between these "dots," suggesting that these repeated regions may be involved in the regulation of gene expression (Fig. 4). The "dots" also appear to be running in the lighter streaks running vertically and horizontally in the dot plot (Fig. 4). These lighter streaks rep-

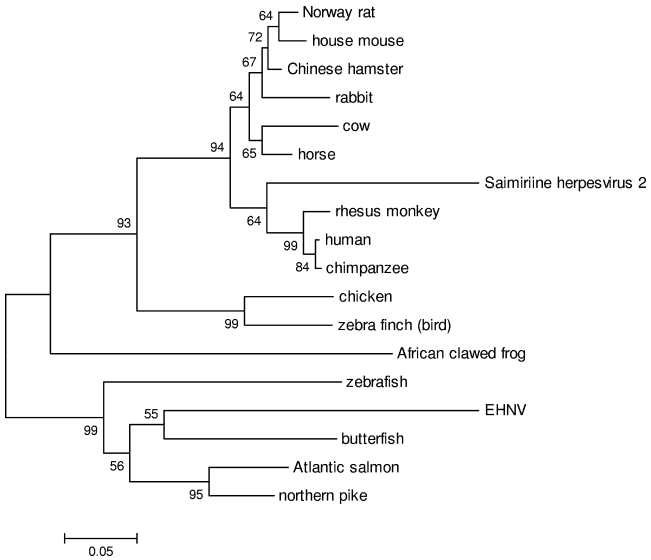

FIG. 2. Phylogenetic analysis of EHNV ORF 87L. Homologous sequences to the EHNV DHFR gene (ORF 87L) were obtained by BLASTP analysis. The neighbor-joining tree was determined using MEGA4, and it is shown with statistical support indicating the robustness of the inferred branching pattern, as assessed using the bootstrap test. The accession number for each gene in the phylogeny is given in Materials and Methods.

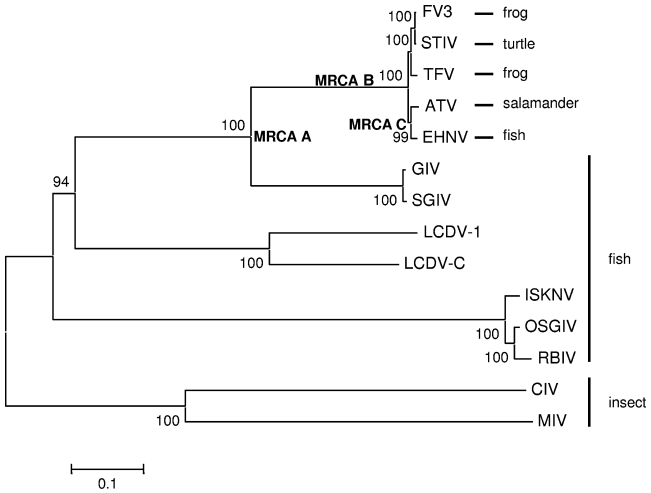

FIG. 3. Concatenated phylogeny of 26 conserved iridovirus sequences. Phylogenetic relationships of 26 conserved open reading frames from the 13 completely sequenced iridovirus genomes are shown. The neighbor-joining tree obtained using MEGA4 is shown, with statistical support indicating the robustness of the inferred branching pattern, as assessed using the bootstrap test. The sequences used for this analysis are described in Tables S1 and S3 in the supplemental material. The most recent common ancestors (MRCAs) are indicated at particular branch points on the phylogeny.

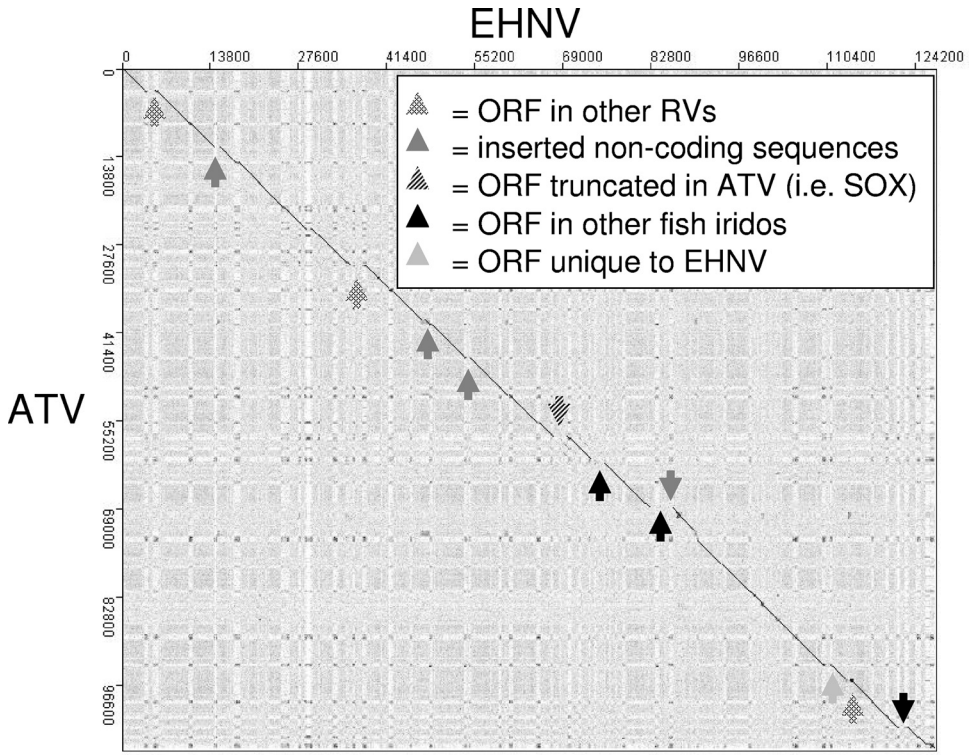

FIG. 4. Dot plot analysis of EHNV versus ATV. The genomic sequence of EHNV was compared to that of ATV by dot plot analysis (JDotter [www.biovirus.org/]). The dot plot comparison of EHNV with ATV shows unique sequences in the EHNV genome.

resent regions of different G/C or A/T content, a phenomenon also observed with poxviruses (11). The EHNV genome has an overall G+C content of 54% (Table 1), but this does not mean that the entire genome has a uniform %GC, as some regions are more G/C rich than others. The A/T-rich regions appear as lighter streaks on the dot plot, with the off-vertical dots indicating similar A/T-rich regions at multiple places in the genomes. Similar patterns have been observed previously in dot plots for ATV, TFV, and FV3 (20, 36, 58).

As observed in other dot plot comparisons (20, 36), the typical RV repeat patterns can be observed by comparing EHNV to ATV, FV3, and TFV (Fig. 4 and 5). Comparing EHNV to ATV by dot plot analysis showed colinearity between these two RVs (Fig. 4). This is a surprising result, as these two viruses infect very different hosts and have been isolated on different continents. This observation suggests that these two different RV pathogens are very closely related, confirming the phylogenetic analysis of 26 ORFs (Fig. 3). There are regions of the dot plot that show unique sequences in EHNV compared to ATV, and these regions correlate with the unique EHNV ORFs (Fig. 4; see Table S1 in the supplemental material) or with extra noncoding DNA sequences. These extra sequences are visualized as breaks in the −45° colinear line and a shift in this line to the right. This shift represents a sequence that is in EHNV but not present in ATV (Fig. 4). There are no sequences present in ATV that are missing from EHNV.

In contrast to previous reports (58), no inversions were observed between FV3 and TFV, using the same program (MacVector) or the dot plot program used in this study (JDotter; data not shown). In addition, dot plots comparing FV3 and STIV revealed colinearity between these two ranaviruses (29), and dot plots comparing SGIV with GIV also revealed complete colinearity, although the starts of these RV genomes differ (data not shown). Therefore, EHNV and ATV, FV3, STIV, and TFV, and SGIV and GIV were each grouped together for dot plot analysis (Fig. 5A and B). Two major genomic inversions in the FV3/TFV lineage compared to the EHNV/ATV lineage can be visualized on the dot plot as a +45° line (Fig. 5A). This is similar to previously published reports comparing FV3/TFV with ATV (20, 36). In comparing EHNV/ATV to GIV/SGIV, long stretches of colinearity are not observed between these sequences, although small sections of colinearity can be observed in the dot plot (Fig. 5B). The short diagonal lines on the dot plot are indicative of groups of ORFs (2 to 4 ORFs) that are scattered throughout the genome, suggesting that major genomic rearrangements have taken place among RV species. The dot plot correlates with the phylogeny in that EHNV is more closely related to the amphibian RVs than it is to the GIV-like viruses that infect fish.

Very little colinearity was observed in comparing EHNV to all other completely sequenced iridovirus isolates (data not shown). Short stretches of colinearity were observed, but the numbers, intensities, and lengths of these lines were much smaller when comparing EHNV to all other iridovirus genomic sequences.

A closer examination of the genomic dot plots between SGIV and EHNV and between SGIV and FV3 revealed additional information on the evolution of the ranaviruses. In Fig. 6A and B, the small stretches of colinear ORFs along the

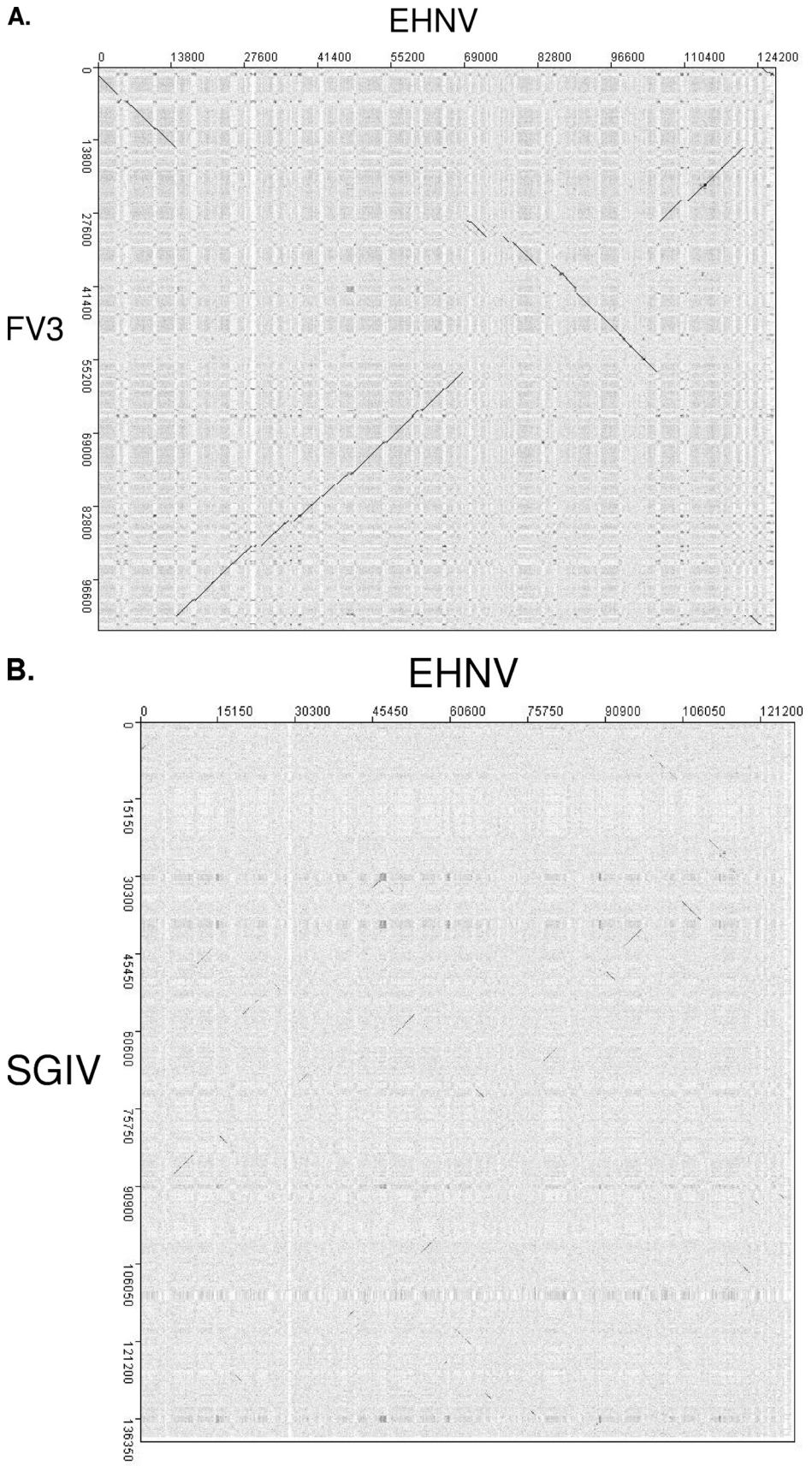

FIG. 5. Dot plot analysis of EHNV versus other ranaviruses. The genomic sequence of EHNV was compared to those of FV3 and SGIV by dot plot analysis (JDotter [www.biovirus.org/]). (A) Comparison of the EHNV genome to the FV3 genome. (B) Dot plot comparison of EHNV and SGIV genomic sequences.

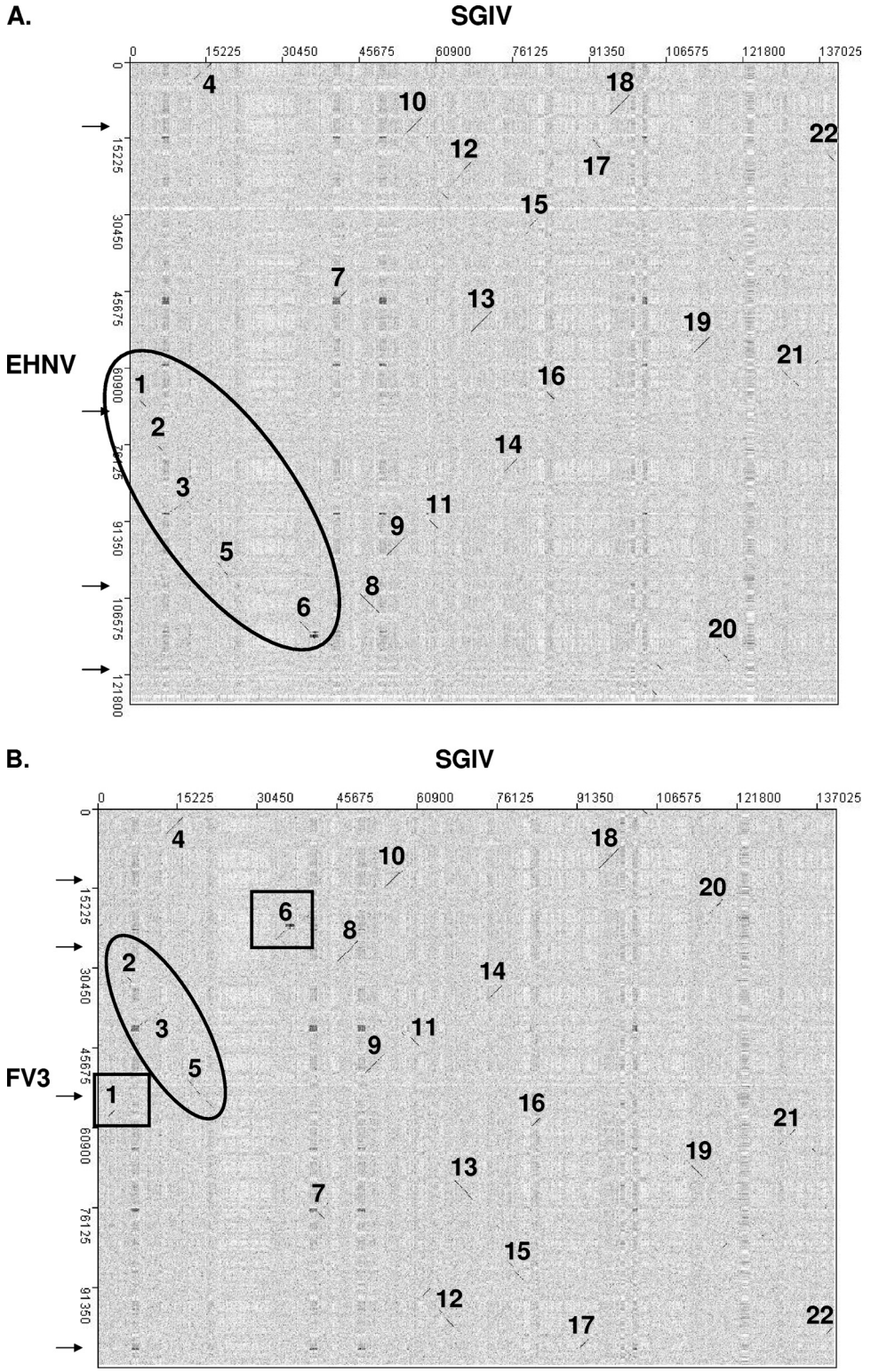

FIG. 6. Dot plot analysis of SGIV compared to EHNV and FV3. Dot plots were generated comparing SGIV to EHNV (A) and FV3 (B). Colinear segments were sequentially numbered along the SGIV genome. Consecutively ordered segments along the EHNV and FV3 genomes are circled, while inverted segments are boxed.

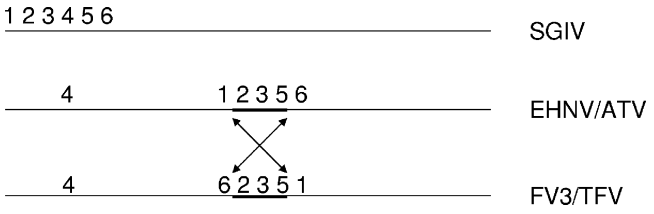

FIG. 7. Model of ranavirus genomic rearrangements. Using the dot plot analysis shown in Fig. 5, consecutively ordered colinear segments were arranged diagrammatically. Comparing the order and orientation of the colinear segments, the rearrangements observed in Fig. 4 occurred in the FV3-like virus lineage and not in the ATV-like virus lineage.

SGIV genome are numbered consecutively. EHNV (and ATV) has segments 1 through 6 oriented together in consecutive order (Fig. 6A). However, the FV3 genome has a rearrangement of these segments (Fig. 6B). This rearrangement of segments corresponds to the inversion observed when comparing the EHNV/ATV and FV3/TFV genomic sequences (Fig. 5A and arrows in Fig. 6). Therefore, these data suggest that in EHNV/ATV, the gene order in this region is similar to the gene order in the most common recent ancestor (MRCA) of the ranaviruses (MRCA A) (Fig. 3) and that the inversion observed when comparing EHNV/ATV and FV3/TFV occurred in the FV3-like lineage (Fig. 7). There is not enough conservation of gene order in the region of the second inver-

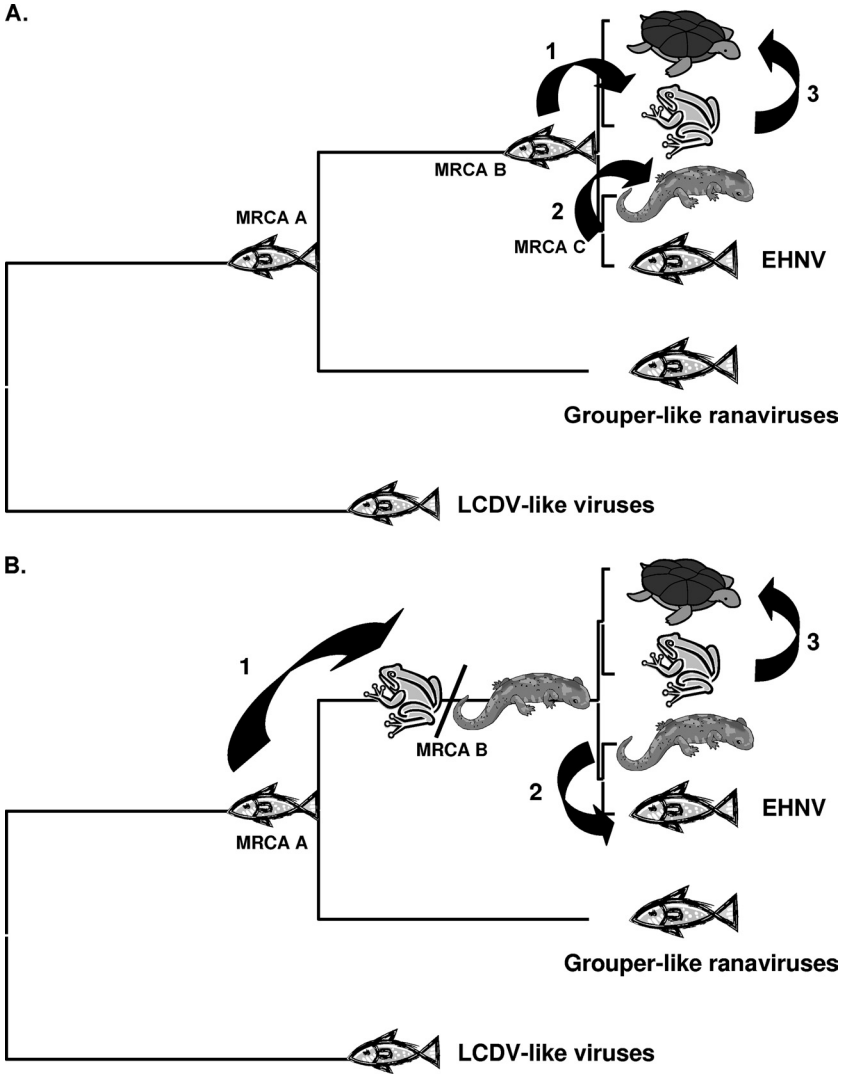

FIG. 8. Ranavirus multiple-species jump hypotheses. Throughout the majority of evolutionary history, the iridoviruses have been restricted to fish species. Based on recent genomic sequence information, we hypothesize that the most recent common ancestor of the ranaviruses was a fish virus (MRCA A). In addition, we hypothesize that there have been evolutionarily recent host shifts. We propose two hypotheses to explain these multiple recent host shifts among the amphibian-like ranaviruses. (A) One hypothesis suggests that the most recent common ancestor of the ALRVs was a fish virus (MRCA B) and that a jump occurred from fish to frogs, with a subsequent jump from frogs to turtles. In addition, if the most recent common ancestor of the ATV-like viruses was a fish virus (MRCA C), then another jump from fish to salamanders occurred. (B) An alternative hypothesis suggests that the most recent common ancestor of the ranaviruses was a fish virus (MRCA A) and that a jump occurred from fish into tetrapod amphibians (MRCA B). At this time, it is unclear if the shift in host species was from fish to frogs, fish to salamanders, or both. A subsequent host shift occurred from frogs to turtles, as well as a jump from salamanders back into fish.

sion to be able to establish if the second inversion occurred in the ATV-like or FV3-like lineage.

Since the ALRVs contain a virus isolated from fish (EHNV) and since all of the more distantly related vertebrate iridoviruses infect fish (GIV/SGIV, LCDV, and ISKNV), we hypothesize that the most recent common ancestor of the ALRVs was an ancestral fish virus (MRCA B) (Fig. 3 and 8A). Thus, an evolutionarily recent host shift from fish to amphibians, surmised by the shallowness of the ALRV branch lengths, must have occurred. In fact, our data suggest that there were two species jumps, one from fish to frogs (MRCA B) and a jump from fish to salamanders (MRCA C) (Fig. 8A). In addition, the rearrangement of the FV3-like virus genomic DNA relative to ATV/EHNV resulted in the speciation of the ALRVs into the ATV-like and FV3-like virus lineages. The newly acquired sequence of the soft-shelled turtle RV, which is completely colinear with FV3 (29), suggests that another host jump, from frogs to reptiles, also took place recently in evolutionary history (Fig. 3 and 8). However, an alternative hypothesis, where the most recent common ancestor for the ALRVs (MRCA B in Fig. 3 and 8B) infected a tetrapod amphibian, such that the species jump from fish to amphibians occurred prior to speciation of the ALRVs, is also consistent with the phylogeny in Fig. 3. This alternative hypothesis would require a more recent jump back from tetrapod amphibians into fish, yielding an EHNV-like virus. Both of these hypotheses suggest that for the majority of evolutionary time vertebrate iridoviruses were confined to fish, and much more recently, there appear to have been at least three species jumps, from fish to frogs, from fish to salamanders, and from frogs to reptiles, and perhaps as many as four species jumps, including a jump from tetrapod amphibians back to fish. It is tempting to speculate that activities associated with human harvesting of aquatic organisms during the past 40,000 years (28, 47, 48) led to the more common recent jumping of ranaviruses among aquatic organisms.

The sequencing of EHNV has allowed us to hypothesize that ranavirus host shifts are possible and that there have been evolutionarily recent ranavirus host shifts. In addition, the ability of this group of viruses to infect such a wide variety of host species suggests that more host shifts are likely. Therefore, it is important that we understand more of the evolutionary traits of this unique group of viruses, as there is no other closely related group of viruses that infect such a broad group of hosts, with the possible exception of the orthomyxoviruses (64).

Infectious diseases have become recognized as one of the most important threats to public, veterinary, and wildlife health over the past 30 years (4, 12). Combating infectious diseases is a key goal of public and veterinary health efforts, both nationally and internationally. Infectious diseases in insects, mammals, marsupials, amphibians, reptiles, and fish are not well understood. Global air travel, trade, tourism, immigration, and expansion of human settlements effectively increase the mixing of pathogens among humans as well as domestic and wild animals. From 1998 to 2000, the most-reported wildlife pathogens were viruses related to the anthropogenic movement of animals (12, 17). Recent reports have suggested that RVs move around the globe in host species used for bait, food, pets, and research (35, 44, 51). This phenomenon may increase the probability of new RV pathogens emerging in naïve populations and supports the need for controlling the movement of RV host species within and between geographical regions. Since RVs infect a wide variety of ecologically and economically important hosts, understanding RV evolution, including the importance of the unique genomic rearrangements found among RV isolates in relation to host specificity and viral evolution, will help to predict and perhaps to prevent further RV epizootics. While this study does give insight into RV evolution, more genomic sequence information is needed to continue our efforts to understand the role that RVs play in the environment.

ACKNOWLEDGMENTS

This work was supported in part by Integrated Research Challenges in Environmental Biology (IBN-9977063) and Division of Environmental Biology (0213851) grants from the National Science Foundation.

REFERENCES

1. **Ahne, W., M. Bearzotti, M. Bremont, and S. Essbauer.** 1989. Comparison of European systemic piscine and amphibian iridoviruses with epizootic haematopoietic necrosis virus and frog virus 3. Zentralbl. Veterinarmed. B **45:**373–383.
2. **Ahne, W., M. Bremont, R. P. Hedrick, A. D. Hyatt, and R. J. Whittington.** 1997. Iridoviruses associated with epizootic haematopoietic necrosis (EHN) in aquaculture. World J. Microbiol. Biotechnol. **13:**367–373.
3. **Allender, M. C., M. M. Fry, A. R. Irizarry, L. Craig, A. J. Johnson, and M. Jones.** 2006. Intracytoplasmic inclusions in circulating leukocytes from an eastern box turtle (Terrapene carolina carolina) with iridoviral infection. J. Wildl. Dis. **42:**677–684.
4. **Binder, S., A. M. Levitt, J. J. Sacks, and J. M. Hughes.** 1999. Emerging infectious diseases: public health issues for the 21st century. Science **284:** 1311–1313.
5. **Bloch, B., and J. L. Larsen.** 1993. An iridovirus-like agent associated with systemic infection in cultured turbot Scophthalmus-maximus fry in Denmark. Dis. Aquat. Organ. **15:**235–240.
6. **Bollinger, T. K., J. Mao, D. Schock, R. M. Brigham, and V. G. Chinchar.** 1999. Pathology, isolation, and preliminary molecular characterization of a novel iridovirus from tiger salamanders in Saskatchewan. J. Wildl. Dis. **35:**413–429.
7. **Bratke, K. A., and A. McLysaght.** 2008. Identification of multiple independent horizontal gene transfers into poxviruses using a comparative genomics approach. BMC Evol. Biol. **8:**67.
8. **Chinchar, V. G.** 2002. Ranaviruses (family Iridoviridae): emerging cold-blooded killers. Arch. Virol. **147:**447–470.
9. **Chinchar, V. G., A. Hyatt, T. Miyazaki, and T. Williams.** 2009. Family Iridoviridae: poor viral relations no longer. Curr. Top. Microbiol. Immunol. **328:**123–170.
10. **Cunningham, A. A., T. E. S. Langton, P. M. Bennett, J. F. Lewin, S. E. N. Drury, R. E. Gough, and S. K. MacGregor.** 1996. Pathological and microbiological findings from incidents of unusual mortality of the common frog (Rana temporaria). Philos. Trans. R. Soc. Lond. B **351:**1539–1557.
11. **Da Silva, M., and C. Upton.** 2005. Host-derived pathogenicity islands in poxviruses. Virol. J. **2:**30.
12. **Daszak, P., A. A. Cunningham, and A. D. Hyatt.** 2000. Emerging infectious diseases of wildlife—threats to biodiversity and human health. Science **287:** 443–449.
13. **Delhon, G., E. R. Tulman, C. L. Afonso, Z. Lu, J. J. Becnel, B. A. Moser, G. F. Kutish, and D. L. Rock.** 2006. Genome of invertebrate iridescent virus type 3 (mosquito iridescent virus). J. Virol. **80:**8439–8449.
14. **De Voe, R., K. Geissler, S. Elmore, D. Rotstein, G. Lewbart, and J. Guy.** 2004. Ranavirus-associated morbidity and mortality in a group of captive eastern box turtles (Terrapene carolina carolina). J. Zoo Wildl. Med. **35:** 534–543.
15. **Do, J. W., C. H. Moon, H. J. Kim, M. S. Ko, S. B. Kim, J. H. Son, J. S. Kim, E. J. An, M. K. Kim, S. K. Lee, M. S. Han, S. J. Cha, M. S. Park, M. A. Park, Y. C. Kim, J. W. Kim, and J. W. Park.** 2004. Complete genomic DNA sequence of rock bream iridovirus. Virology **325:**351–363.
16. **Dobrindt, U., B. Hochhut, U. Hentschel, and J. Hacker.** 2004. Genomic islands in pathogenic and environmental microorganisms. Nat. Rev. Microbiol. **2:**414–424.
17. **Dobson, A., and J. Foufopoulos.** 2001. Emerging infectious pathogens of wildlife. Philos. Trans. R. Soc. Lond. B **356:**1001–1012.
18. **Donnelly, T. M., E. W. Davidson, J. K. Jancovich, S. Borland, M. Newberry, and J. Gresens.** 2003. What's your diagnosis? Ranavirus infection. Lab. Anim. (New York) **32:**23–25.

19. **Drury, S. E. N., R. E. Gough, and A. A. Cunningham.** 1995. Isolation of an iridovirus-like agent from common frogs (Rana-temporaria). Vet. Rec. **137:** 72–73.
20. **Eaton, H. E., J. Metcalf, E. Penny, V. Tcherepanov, C. Upton, and C. R. Brunetti.** 2007. Comparative genomic analysis of the family Iridoviridae: re-annotating and defining the core set of iridovirus genes. Virol. J. **4:**11.
21. **Gerlach, R. G., and M. Hensel.** 2007. Salmonella pathogenicity islands in host specificity host pathogen-interactions and antibiotic resistance of Salmonella enterica. Berl. Munch. Tierarztl. Wochenschr. **120:**317–327.
22. **Gerlach, R. G., D. Jackel, B. Stecher, C. Wagner, A. Lupas, W. D. Hardt, and M. Hensel.** 2007. Salmonella pathogenicity island 4 encodes a giant non-fimbrial adhesin and the cognate type 1 secretion system. Cell. Microbiol. **9:**1834–1850.
23. **Gordon, D., C. Abajian, and P. Green.** 1998. Consed: a graphical tool for sequence finishing. Genome Res. **8:**195–202.
24. **Greer, A. L., M. Berrill, and P. J. Wilson.** 2005. Five amphibian mortality events associated with ranavirus infection in south central Ontario, Canada. Dis. Aquat. Organ. **67:**9–14.
25. **Hacker, J., B. Hochhut, B. Middendorf, G. Schneider, C. Buchrieser, G. Gottschalk, and U. Dobrindt.** 2004. Pathogenomics of mobile genetic elements of toxigenic bacteria. Int. J. Med. Microbiol. **293:**453–461.
26. **He, J. G., M. Deng, S. P. Weng, Z. Li, S. Y. Zhou, Q. X. Long, X. Z. Wang, and S. M. Chan.** 2001. Complete genome analysis of the mandarin fish infectious spleen and kidney necrosis iridovirus. Virology **291:**126–139.
27. **He, J. G., L. Lu, M. Deng, H. H. He, S. P. Weng, X. H. Wang, S. Y. Zhou, Q. X. Long, X. Z. Wang, and S. M. Chan.** 2002. Sequence analysis of the complete genome of an iridovirus isolated from the tiger frog. Virology **292:**185–197.
28. **Hu, Y. W., H. Shang, H. W. Tong, O. Nehlich, W. Liu, C. H. Zhao, J. C. Yu, C. S. Wang, E. Trinkaus, and M. P. Richards.** 2009. Stable isotope dietary analysis of the Tianyuan 1 early modern human. Proc. Natl. Acad. Sci. USA **106:**10971–10974.
29. **Huang, Y. H., X. H. Huang, H. Liu, J. Gong, Z. L. Ouyang, H. C. Cui, J. H. Cao, Y. T. Zhao, X. J. Wang, Y. L. Jiang, and Q. W. Qin.** 2009. Complete sequence determination of a novel reptile iridovirus isolated from soft-shelled turtle and evolutionary analysis of Iridoviridae. BMC Genomics **10:**224–238.
30. **Hyatt, A. D., M. Williamson, B. E. H. Coupar, D. Middleton, S. G. Hengstberger, A. R. Gould, P. Selleck, T. G. Wise, J. Kattenbelt, A. A. Cunningham, and J. Lee.** 2002. First identification of a ranavirus from green pythons (Chondropython viridis). J. Wildl. Dis. **38:**239–252.
31. **Iyer, L. A., S. Balaji, E. V. Koonin, and L. Aravind.** 2006. Evolutionary genomics of nucleo-cytoplasmic large DNA viruses. Virus Res. **117:**156–184.
32. **Iyer, L. M., L. Aravind, and E. V. Koonin.** 2001. Common origin of four diverse families of large eukaryotic DNA viruses. J. Virol. **75:**11720–11734.
33. **Jakob, N. J., K. Muller, U. Bahr, and G. Darai.** 2001. Analysis of the first complete DNA sequence of an invertebrate iridovirus: coding strategy of the genome of Chilo iridescent virus. Virology **286:**182–196.
34. **Jancovich, J. K., E. W. Davidson, J. F. Morado, B. L. Jacobs, and J. P. Collins.** 1997. Isolation of a lethal virus from the endangered tiger salamander Ambystoma tigrinum stebbinsi. Dis. Aquat. Organ. **31:**161–167.
35. **Jancovich, J. K., E. W. Davidson, N. Parameswaran, J. Mao, V. G. Chinchar, J. P. Collins, B. L. Jacobs, and A. Storfer.** 2005. Evidence for emergence of an amphibian iridoviral disease because of human-enhanced spread. Mol. Ecol. **14:**213–224.
36. **Jancovich, J. K., J. Mao, V. G. Chinchar, C. Wyatt, S. T. Case, S. Kumar, G. Valente, S. Subramanian, E. W. Davidson, J. P. Collins, and B. L. Jacobs.** 2003. Genomic sequence of a ranavirus (family Iridoviridae) associated with salamander mortalities in North America. Virology **316:**90–103.
37. **Johnson, A. J., A. P. Pessier, and E. R. Jacobson.** 2007. Experimental transmission and induction of ranaviral disease in western ornate box turtles (Terrapene ornata ornata) and red-eared sliders (Trachemys scripta elegans). Vet. Pathol. **44:**285–297.
38. **Langdon, J. S., J. D. Humphrey, and L. M. Williams.** 1988. Outbreaks of an EHNV-like iridovirus in cultured rainbow-trout, Salmo-gairdneri richardson, in Australia. J. Fish Dis. **11:**93–96.
39. **Langdon, J. S., J. D. Humphrey, L. M. Williams, A. D. Hyatt, and H. A. Westbury.** 1986. 1st virus isolation from Australian fish—an iridovirus-like pathogen from redfin perch, Perca-fluviatilis L. J. Fish Dis. **9:**263–268.
40. **Lu, L., S. Y. Zhou, C. Chen, S. P. Weng, S. M. Chan, and J. G. He.** 2005. Complete genome sequence analysis of an iridovirus isolated from the orange-spotted grouper, Epinephelus coioides. Virology **339:**81–100.
41. **Mao, J. H., R. P. Hedrick, and V. G. Chinchar.** 1997. Molecular characterization, sequence analysis, and taxonomic position of newly isolated fish iridoviruses. Virology **229:**212–220.
42. **Marschang, R. E., P. Becher, H. Posthaus, P. Wild, H. J. Thiel, U. Muller-Doblies, E. F. Kalet, and L. N. Bacciarini.** 1999. Isolation and characterization of an iridovirus from Hermann's tortoises (Testudo hermanni). Arch. Virol. **144:**1909–1922.
43. **Marschang, R. E., S. Braun, and P. Becher.** 2005. Isolation of a ranavirus from a gecko (Uroplatus fimbriatus). J. Zoo Wildl. Med. **36:**295–300.
44. **Picco, A. M., and J. P. Collins.** 2008. Amphibian commerce as a likely source of pathogen pollution. Conserv. Biol. **22:**1582–1589.
45. **Pozet, F., M. Morand, A. Moussa, C. Torhy, and P. Dekinkelin.** 1992. Isolation and preliminary characterization of a pathogenic icosahedral deoxyribovirus from the catfish Ictalurus-melas. Dis. Aquat. Organ. **14:**35–42.
46. **Qin, Q. W., S. F. Chang, G. H. Ngoh-Lim, S. Gibson-Kueh, C. Shi, and T. J. Lam.** 2003. Characterization of a novel ranavirus isolated from grouper Epinephelus tauvina. Dis. Aquat. Organ. **53:**1–9.
47. **Richards, M. P., P. B. Pettitt, M. C. Stiner, and E. Trinkaus.** 2001. Stable isotope evidence for increasing dietary breadth in the European mid-Upper Paleolithic. Proc. Natl. Acad. Sci. USA **98:**6528–6532.
48. **Richards, M. P., and E. Trinkaus.** 2009. Isotopic evidence for the diets of European Neanderthals and early modern humans. Proc. Natl. Acad. Sci. USA **106:**16034–16039. doi:10.1073/pnas.0903821106.
49. **Schaffer, A. A., L. Aravind, T. L. Madden, S. Shavirin, J. L. Spouge, Y. I. Wolf, E. V. Koonin, and S. F. Altschul.** 2001. Improving the accuracy of PSI-BLAST protein database searches with composition-based statistics and other refinements. Nucleic Acids Res. **29:**2994–3005.
50. **Schaffer, A. A., Y. I. Wolf, C. P. Ponting, E. V. Koonin, L. Aravind, and S. F. Altschul.** 1999. IMPALA: matching a protein sequence against a collection of PSI-BLAST-constructed position-specific score matrices. Bioinformatics **15:**1000–1011.
51. **Schloegal, L. M., A. M. Picco, A. M. Kilpatrick, A. J. Davies, and A. D. Hyatt.** 2009. Magnitude of the US trade in amphibians and presence of *Batrachochytrium dendrobatidis* and ranavirus infection in imported North American bullfrogs (*Rana catesbeiana*). Biol. Conserv. **142:**1420–1426.
52. **Schock, D. M., T. K. Bollinger, V. G. Chinchar, J. K. Jancovich, and J. P. Collins.** 2008. Experimental evidence that amphibian ranaviruses are multi-host pathogens. Copeia **2008:**133–143.
53. **Song, W. J., Q. W. Qin, J. Qiu, C. H. Huang, F. Wang, and C. L. Hew.** 2004. Functional genomics analysis of Singapore grouper iridovirus: complete sequence determination and proteomic analysis. J. Virol. **78:**12576–12590.
54. **Sonnhammer, E. L. L., and R. Durbin.** 1995. A dot-matrix program with dynamic threshold control suited for genomic DNA and protein-sequence analysis. Gene **167:**GC1–GC10.
55. **Sonnhammer, E. L. L., and J. C. Wootton.** 2001. Integrated graphical analysis of protein sequence features predicted from sequence composition. Proteins **45:**262–273.
56. **Speare, R., and J. R. Smith.** 1992. An iridovirus-like agent isolated from the ornate burrowing frog Limnodynastes-ornatus in Northern Australia. Dis. Aquat. Organ. **14:**51–57.
57. **Tamura, K., J. Dudley, M. Nei, and S. Kumar.** 2007. MEGA4: molecular evolutionary genetics analysis (MEGA) software version 4.0. Mol. Biol. Evol. **24:**1596–1599.
58. **Tan, W. G. H., T. J. Barkman, V. G. Chinchar, and K. Essani.** 2004. Comparative genomic analyses of frog virus 3, type species of the genus Ranavirus (family Iridoviridae). Virology **323:**70–84.
59. **Tapiovaara, H., N. J. Olesen, J. Linden, E. Rimaila-Parnanen, and C. H. von Bonsdorff.** 1998. Isolation of an iridovirus from pike-perch Stizostedion lucioperca. Dis. Aquat. Organ. **32:**185–193.
60. **Tidona, C. A., and G. Darai.** 1997. The complete DNA sequence of lymphocystis disease virus. Virology **230:**207–216.
61. **Trimble, J. J., S. C. S. Murthy, A. Bakker, R. Grassmann, and R. C. Desrosiers.** 1988. A gene for dihydrofolate-reductase in a herpesvirus. Science **239:**1145–1147.
62. **Tsai, C. T., J. W. Ting, M. H. Wu, M. F. Wu, I. C. Guo, and C. Y. Chang.** 2005. Complete genome sequence of the grouper iridovirus and comparison of genomic organization with those of other iridoviruses. J. Virol. **79:**2010–2023.
63. **Whittington, R. J., C. Kearns, A. D. Hyatt, S. Hengstberger, and T. Rutzou.** 1996. Spread of epizootic haematopoietic necrosis virus (EHNV) in redfin perch (Perca fluviatilis) in southern Australia. Aust. Vet. J. **73:**112–114.
64. **Williams, T., V. Barbosa-Solomieu, and V. G. Chinchar.** 2005. A decade of advances in iridovirus research. Adv. Virus Res. **65:**173–248.
65. **Yu, Y. X., M. Bearzotti, P. Vende, W. Ahne, and M. Bremont.** 1999. Partial mapping and sequencing of a fish iridovirus genome reveals genes homologous to the frog virus 3 p31, p40 and human eIF2 alpha. Virus Res. **63:**53–63.
66. **Zhang, Q. Y., F. Xiao, Z. Q. Li, J. F. Gui, J. H. Mao, and V. G. Chinchar.** 2001. Characterization of an iridovirus from the cultured pig frog Rana grylio with lethal syndrome. Dis. Aquat. Organ. **48:**27–36.
67. **Zhang, Q. Y., F. Xiao, J. Xie, Z. Q. Li, and J. F. Gui.** 2004. Complete genome sequence of lymphocystis disease virus isolated from China. J. Virol. **78:** 6982–6994.
68. **Zupanovic, Z., C. Musso, G. Lopez, C. L. Louriero, A. D. Hyatt, S. Hengstberger, and A. J. Robinson.** 1998. Isolation and characterization of iridoviruses from the giant toad Bufo marinus in Venezuela. Dis. Aquat. Organ. **33:**1–9.